AIP | Journal of Applied Physics

Lorentz-force dependence of the critical current for SmBCO coated conductor

Sangjun Oh, Chulhee Lee, Kyuhwan Cho, Sangmoo Lee, and Dojun Youm

Citation: J. Appl. Phys. **104**, 083913 (2008); doi: 10.1063/1.3000627
View online: http://dx.doi.org/10.1063/1.3000627
View Table of Contents: http://jap.aip.org/resource/1/JAPIAU/v104/i8
Published by the American Institute of Physics.

Lorentz-force dependence of the critical current for SmBCO coated conductor

Sangjun Oh,[1,a)] Chulhee Lee,[1] Kyuhwan Cho,[1] Sangmoo Lee,[2] and Dojun Youm[2]
[1]*Material Research Team, National Fusion Research Institute, 52 Eoeun-dong, Yuseong, Daejeon 305-333, Republic of Korea*
[2]*Department of Physics, Korea Advanced Institute of Science and Technology, 335 Gwahangno, Yuseong, Daejeon 305-701, Republic of Korea*

(Received 8 June 2008; accepted 30 August 2008; published online 24 October 2008)

Angular dependence of the critical current in a varying Lorentz-force configuration for a SmBCO coated conductor has been studied. Near the transition temperature, the angular dependence of the critical current in a varying Lorentz-force configuration was quite similar to the result of a constant Lorentz-force measurement. As the temperature is lowered and as the field is aligned along the *ab*-plane, the critical current measured in a varying Lorentz-force configuration becomes larger than the constant Lorentz-force measurement. We found that the field dependence of the critical current and *n*-value can be described by the same pinning model, the Kramer model including thermal activation, reported for constant Lorentz-force measurements of various ReBCO (Re, rare earth, Sm, or Y) thin films [S. Oh *et al.*, J. Appl. Phys. **102**, 043904 (2007)]. As a possible reason, the Lorentz force acting on segments of twisted vortex lines due to collective pinning or by thermal excitations is discussed. It is further argued that the difference in the critical current for the varying and constant Lorentz-force measurements can be understood as mainly due to a variation in the pinning force, if we interpret the Lorentz force on twisted vortex lines as a scalar product between the applied field and current. © *2008 American Institute of Physics*. [DOI: 10.1063/1.3000627]

It is well established that the critical current of type II superconductor is determined by a balance between the Lorentz force and the pinning force. For example, the critical current of Nb_3Sn can be calculated and estimated from scaling law for flux pinning, which is based on the equivalence of the pinning force and the Lorentz force.[1] On the other hand, for high T_c cuprate superconductors, the relation between the Lorentz force and the pinning force is a bit dubious. Soon after the discovery of cuprate superconductors, giant resistive broadening is observed, which is known to be Lorentz-force independent and strongly related with superconducting fluctuation.[2] The critical current measurements under various applied field configurations did not give conclusive results either. The critical current measurements under field aligned in a varying Lorentz-force (VLF) configuration [Fig. 1(a)] are quite different from what we can expect from the results of constant Lorentz-force (CLF) measurements [Fig. 1(b)] on the basis of Lorentz-force dependence.[3–6] The Lorentz-force dependence of the critical current was only indirectly claimed either from an additional peak in the angular dependence of the critical current for the field direction along the *c*-axis[5] or from the modified Anderson–Kim critical state model and its relevance with the measured angular dependence of the critical current.[4]

In our previous work, we showed that the angular dependence of the critical current with field aligned in a CLF configuration can be understood by the Kramer model including thermal activation, where the critical current is determined by a balance between the Lorentz force and the pinning force dominated by the flux line lattice shearing.[7] The model reasonably fits the data for a variety of ReBCO (Re, rare earth, Sm, or Y) thin films even if there is another maximum in the angular dependence of the critical current when the field is aligned along the *c*-axis. In this work, we measure the critical currents for a $Sm_1Ba_2Cu_3O_7$ (SmBCO) coated conductor in a VLF configuration and compared with the results of CLF measurement. The applicability of the Kramer model including thermal activation for the VLF measurement is examined and its meaning on the Lorentz-force dependence of the critical current is further discussed.

The angular dependence of the critical current for a SmBCO coated conductor in a VLF configuration is shown in Fig. 2. The angular dependence of the critical current in a CLF configuration reported in our previous work is drawn together for comparison. $Sm_1Ba_2Cu_3O_7$ thin film was deposited on a textured Ni tape using $CeO_2/YSZ/CeO_2$ buffer layer. The critical current was measured using the horizontal rotator of Quantum Design physical property measurement system. External current source and nanovoltmeter, Keithley 220 and Hewlett-Packard 34420A, were used for the measurements. Detailed measurement methods were reported in our previous work.[7] Very near the transition temperature, at

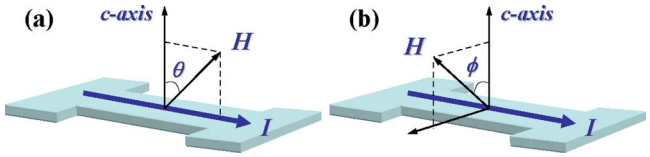

FIG. 1. (Color online) Schematic diagrams of measurement configuration. (a) A VLF configuration. (b) A CLF configuration.

[a)]Author to whom correspondence should be addressed. Electronic mail: wangpi@nfri.re.kr.

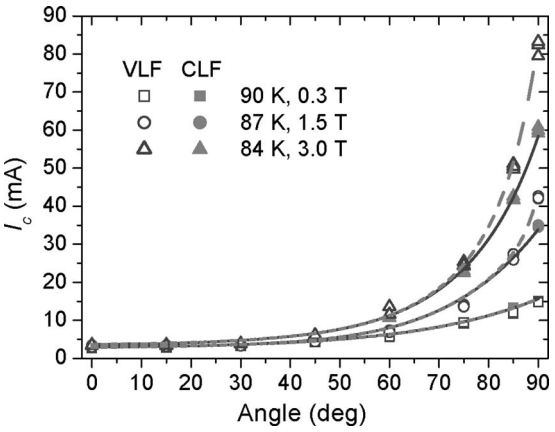

FIG. 2. The angular dependence of the critical current measured in the VLF configuration. The CLF measurement results are drawn together for comparison. Lines are calculated with the Kramer model including thermal activation.

90 K, the difference in the critical current for each configuration is quite negligible, as can be seen in Fig. 2. As temperature is lowered, the critical current measured in the VLF configuration becomes larger than the critical current measured in the CLF configuration, as the angle approaches 90°, as the field is aligned along the *ab*-plane. At 87 K, the critical current starts to deviate when the angle is larger than 85°. As temperature is further lowered, the angle at which the critical current for each configuration starts to deviate from each other is decreased. At 84 K, the critical currents are different for the angle greater than 75°. These features are not unique at the specified field shown in Fig. 2 but universal at other fields as well, as can be seen in Fig. 3.

In our previous work, it was argued that the critical current of various ReBCO thin films measured in the CLF configuration can be understood by the Kramer model, the flux line lattice shearing model, if we include the effect of thermal activation[7]

$$I_c \times B = \left(1 - \exp\left[-\frac{n(B,T,\theta)-1}{n(0,0,\theta)-1}\right]\right) \Big/ (1-e^{-1}) \cdot F_m(T,\theta) f(b), \quad (1)$$

where F_m is the pinning force maximum and b is the reduced field, a ratio between the applied field and the upper critical field B_{c2}. If overall pinning is dominated by the flux line lattice shearing, $f(b)$ can be expressed as $f(b)=b^{1/2}(1-b)^2$.[8] The n-value defined from an empirical power law in the I-V curve is related with the activation energy as $n=U_0/k_BT$.[9] It was further shown that the field dependence of the n-value for a variety of ReBCO thin films can be expressed by the following empirical expression:[7]

$$n(B,T,\theta) = a(T,\theta)[1 - B/B_{\mathrm{irr}}(T,\theta)]^{\nu(T,\theta)} + 1, \quad (2)$$

where a, ν, and B_{irr} are the fitting parameters. If the applied field is equal to B_{irr}, the n-value is 1, the I-V characteristic becomes simple resistive, and the critical current vanishes. The fitting parameter B_{irr} corresponds to the irreversibility field. One of the unique features of the above scaling law of flux pinning for ReBCO thin films is that the upper critical field and the irreversibility field are fitted separately.

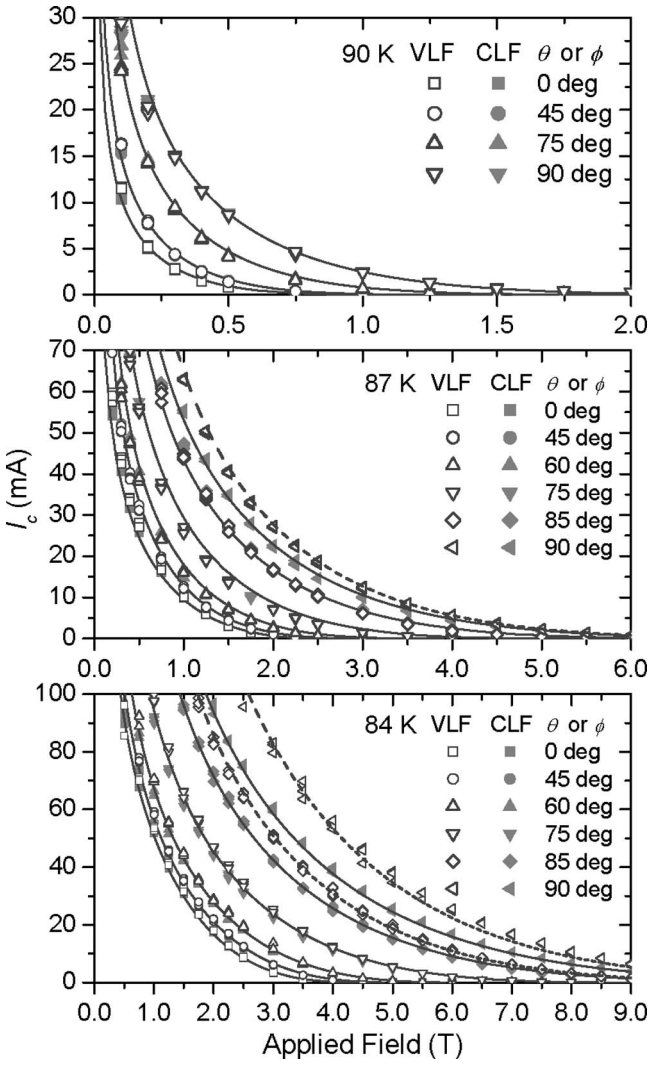

FIG. 3. The field dependence of the critical current measured in the VLF and CLF configurations. Lines are calculated with Eqs. (1) and (2).

The above correlation between the n-value and the critical current can be seen in Figs. 4 and 5, where the field dependence of the critical current is presented in the form of Kramer plots, the field dependence of $I_c^{1/2} \times B^{1/4}$. The difference in the field dependence of the n-value measured in the VLF and CLF was negligible or quite small whether there was a substantial difference in the critical current or not. First, the n-value data were fitted with Eq. (2), and then using the field dependence of the n-value, the field dependence of the critical current was analyzed. All lines in Figs. 4 and 5 calculated with Eqs. (1) and (2) were in agreement with the measurement results. The fitting results (solid lines in Figs. 4 and 5) and parameters for the CLF measurements were discussed in our previous work.[7]

It should be noted that even for the VLF configuration, the field dependences of the critical current and the n-value are in agreement with the same pinning model, the Kramer model including thermal activation, as for the case of CLF measurements. According to collective pinning theory, the pinning force on a segment of vortex line of length L is proportional to $L^{1/2}$, whereas the Lorentz force increases with L. The vortex line elastically deforms itself around random

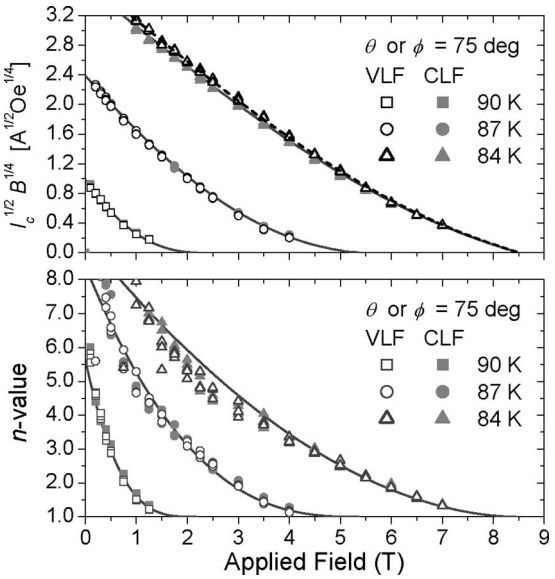

FIG. 4. The Kramer plots and the field dependence of the *n*-value measured in the VLF and CLF configurations. Lines are calculated with Eqs. (1) and (2).

pinning centers to find optimal pinning potential.[10] An example of vortex line aligned along with tilted applied field is depicted in Fig. 6(a). The vortex was usually envisaged as a linear connection of pancake vortex as shown in the left side of Fig. 6(a).[4,11] If we consider the collective pinning, then the vortex line can be twisted [right side of Fig. 6(a)]. The number of segments affected by the Lorentz force for the VLF configuration can be effectively the same as for the case of CLF. [The right side of Fig. 6(a) is a rather exaggerated depiction not considering the collective pinning length.] In such a case, the critical currents measured in the VLF and CLF configurations can be almost equal to each other for most of the angle as shown in Figs. 2 and 3, even if the critical current is determined by a balance between the Lorentz force and the pinning force.

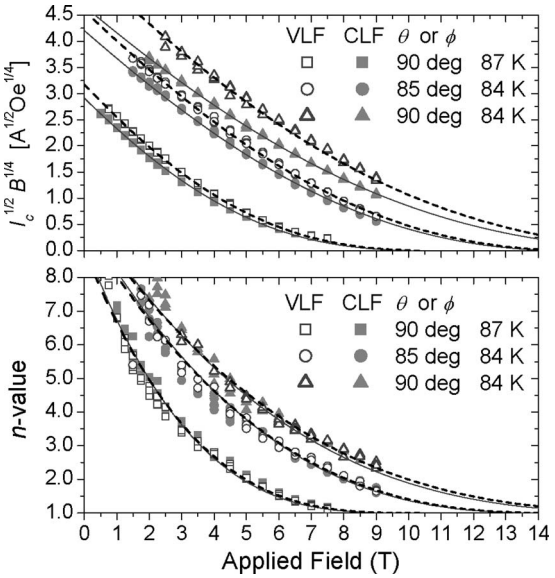

FIG. 5. The Kramer plots and the field dependence of the *n*-value measured in the VLF and CLF configurations. Lines are calculated with Eqs. (1) and (2).

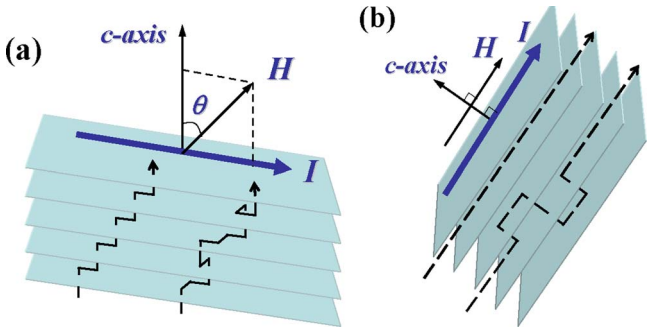

FIG. 6. (Color online) (a) Vortex lines under tilted magnetic field. (b) Vortex lines with field aligned along the *ab*-plane.

As the field is aligned along the *ab*-plane, strong intrinsic pinning starts to dominate and the critical current measured in the VLF configuration becomes larger than the CLF measurement. At 90° in the VLF configuration, the magnetic field is parallel to the applied current and the Lorentz force should vanish [Fig. 6(b)]. For low temperature superconductors, the critical current measured in a parallel magnetic field is usually described by the flux cutting model and is about orders of magnitude higher than that measured in a perpendicular field.[12] However, for the SmBCO coated conductor, the difference in the critical currents measured with the parallel and perpendicular field is rather small and almost vanishes near the transition temperature. This discrepancy may be understood by the excitations of a vortex line such as half-loop or double kink excitation [right side of Fig. 6(b)].[10] As temperature approaches the transition temperature, more excitations are generated. The segments of excitation orthogonal to the current can move easily compared with the intrinsically pinned segments. The critical current may be determined by a balance between the Lorentz force and the pinning force of these segments.

The Lorentz force on a single vortex can be written as $\boldsymbol{f}_L = \boldsymbol{j} \times \boldsymbol{\varphi}$.[10] Here $\boldsymbol{\varphi}$ is the flux contained in a vortex line, which equals a flux quantum. When vortex lines are aligned in a linear way as shown in the left sides of Figs. 6(a) and 6(b), the overall Lorentz force density can be written as $\boldsymbol{F}_L = n\boldsymbol{f}_L = \boldsymbol{j} \times n\boldsymbol{\varphi} = \boldsymbol{j} \times \boldsymbol{B}$, where n is the density of vortex lines.[13] If vortex lines are twisted as depicted in the right sides of Figs. 6(a) and 6(b), we need to consider the segments affected by the Lorentz force, and the overall Lorentz-force density no longer can be written as $\boldsymbol{F}_L = \boldsymbol{j} \times \boldsymbol{B}$. The number of segments affected by the Lorentz force must be strongly temperature dependent, which results in different angular dependences of the critical current in the VLF configuration compared with the results of CLF measurement as shown in Figs. 2 and 3. To a good approximation, at least near the transition temperature, the overall Lorentz force can be written as a scalar product of the applied current and field. In Figs. 4 and 5, the field dependence of the critical current presented in the form of Kramer plots, $I_c^{1/2} B^{1/4}$, was calculated without $(\sin\theta)^{1/2}$ term for the VLF configuration data. It was analyzed with Eqs. (1) and (2) where the left-hand side of Eq. (1), $I_c \times B$ was treated as a scalar product $I_c B$, not as a vector product $I_c B \sin\theta$.

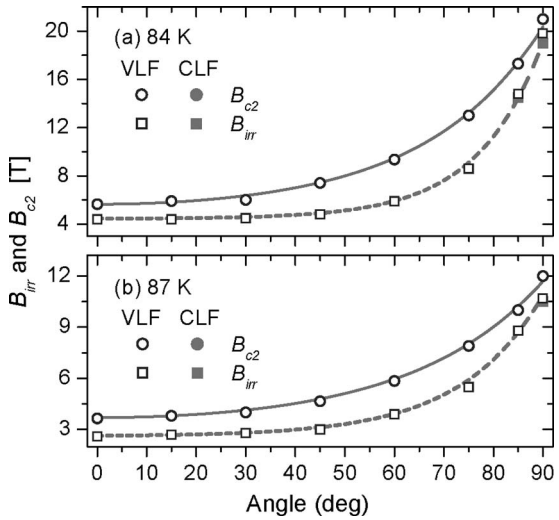

FIG. 7. The angular dependence of the fitting parameters, B_{c2} and B_{irr}, for both the VLF and CLF measurements. Solid lines are calculated with the quasi-2D model of Tinkham and dotted lines are calculated with an empirical expression $c_0+c_1\exp(c_2\theta)$.

The fitting parameters used for the analysis of the VLF data are shown in Figs. 7 and 8. The same upper critical field was used for the analysis of the VLF data as for the fitting of the CLF measurements, of which angular dependence can be described by the quasi-two-dimensional (2D) model of Tinkham,[14]

$$\frac{|B_{c2}(\theta)\cos(\theta)|}{B_{c2,c}}+\left(\frac{B_{c2}(\theta)\sin(\theta)}{B_{c2,ab}}\right)^2=1, \tag{3}$$

where $B_{c2,c}$ and $B_{c2,ab}$ are the upper critical field along the *c*-axis and the *ab*-plane, respectively. Solid lines in Fig. 7 were calculated with Eq. (3). As was discussed in our previous work, there is a bit of uncertainty in the determination of the irreversibility field B_{irr}. The overall VLF data were better fitted with a slightly increased value of B_{irr} compared with the irreversibility field for the CLF measurements as the temperature is lowered and the angle approaches 90° as shown in Fig. 7. On the other hand, the pinning force maximum for the VLF measurements sharply increases at lower temperature and near 90° as presented in Fig. 8, similar to the angular dependence of the critical current itself shown in Fig. 2. Within the scheme of present analysis, the difference in the angular dependence of the critical current between the VLF and CLF configurations can be interpreted as mostly related with the change in the pinning force even though there is a slight increase in the irreversibility field for the VLF measurements.

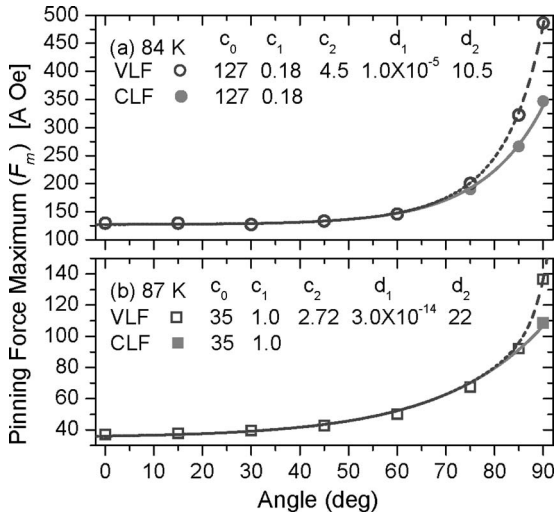

FIG. 8. The angular dependence of the pinning force maximum F_m for both the VLF and CLF measurements. Solid and dotted lines are calculated with empirical expressions $c_0+c_1\exp(c_2\theta)$ and $c_0+c_1\exp(c_2\theta)+d_1\exp(d_2\theta)$, respectively.

The angular dependence of the pinning force maximum for the CLF measurements was fitted by an empirical exponential function $c_0+c_1\exp(c_2\theta)$ in our previous report (solid lines in Fig. 8).[7] We found that the pinning force maximum for the VLF measurements can be fitted by a slightly modified function $c_0+c_1\exp(c_2\theta)+d_1\exp(d_2\theta)$, as shown in Fig. 8 as dotted lines with the fitting parameters presented in the inset. Using the above empirical angular dependence of the pinning force maximum and the other fitting parameters discussed in our previous work, the angular dependence of the critical current also can be calculated as shown in Fig. 2 even for the VLF measurements. The present scheme of analysis based on a representation of the Lorentz force as a scalar product of the applied current and field may be useful for engineering application where the field is applied in an arbitrary direction.

In summary, we have measured the critical current and the *n*-value for a SmBCO coated conductor in a VLF configuration. Negligible difference in the angular dependence of the critical current between the VLF and CLF measurements was observed near the transition temperature. The critical current in a VLF configuration starts to deviate from the result of the CLF measurement, as the temperature is lowered, as the field is aligned along the *ab*-plane. The *n*-value measured in the VLF and CLF configurations was quite similar to each other whether there was a substantial difference in the critical current or not.

The Lorentz-force dependence of the critical current is claimed from the observed similarity in the field dependence of the critical current and *n*-value for both the VLF and CLF measurements. The field dependence of the critical current and *n*-value can be described by the same pinning model, the Kramer model including thermal activation. It is argued that if vortex lines are twisted due to collective pinning, the number of segments affected by the Lorentz force can be effectively the same with each other, results in similar critical current observed for most of the angle. Even if the field and the current are aligned parallel to each other along the *ab*-plane parallel, there can be segments of vortex lines orthogonal to the applied current by excitations such as half-loop or double kink excitation. It is shown that the enhancement in the critical current for the VLF measurement compared with the CLF measurement is mostly related to the sharp increase in the pinning force, if we interpret the Lorentz force on twisted vortex lines as a scalar product between the applied field and current. Using the empirical angular dependence of the pinning force maximum and the other fitting parameters, the angular dependence of the critical cur-

rent can be calculated even for the VLF measurements, which will be beneficial for engineering applications.

This work was supported by the Korea Science and Engineering Foundation (KOSEF) grant funded by the Korean Government (MEST) (Grant No. R01-2007-000-20462-0).

[1]S. Oh and K. Kim, J. Appl. Phys. **99**, 033909 (2006); A. Godeke, B. ten Haken, H. H. J. ten Kate, and D. C. Larbalestier, Supercond. Sci. Technol. **19**, R100 (2006).
[2]K. Kadowaki, Y. Songliu, and K. Kitazawa, Supercond. Sci. Technol. **7**, 519 (1994).
[3]T. Nishizaki, T. Aomine, I. Fujii, K. Yamamoto, S. Yoshii, T. Terashima, and Y. Bando, Physica C **181**, 223 (1991).
[4]T. Nishizaki, F. Ichikawa, T. Fukami, T. Terashima, and Y. Bando, Physica C **204**, 305 (1993).
[5]H. Safar, J. Y. Coulter, M. P. Maley, S. Foltyn, P. Arendt, X. D. Wu, and J. O. Willis, Phys. Rev. B **52**, R9875 (1995).
[6]T. Horide, K. Matsumoto, Y. Yoshida, M. Mukaida, A. Ichinose, S. Horii, and K. Osamura, Jpn. J. Appl. Phys., Part 2 **44**, L111 (2005).
[7]S. Oh, H. Choi, C. Lee, S. Lee, J. Yoo, D. Youm, H. Yamada, and H. Yamasaki, J. Appl. Phys. **102**, 043904 (2007).
[8]E. J. Kramer, J. Appl. Phys. **44**, 1360 (1973).
[9]A. D. Caplin, Y. Bugoslavsky, L. F. Cohen, and G. K. Perkins, Physica C **401**, 1 (2004); S. Oh, C. Lee, K. W. Cho, K. Kim, D. Uglietti, and R. Flukiger, Supercond. Sci. Technol. **20**, 852 (2007).
[10]G. Blatter, M. V. Feigelman, V. B. Geshkenbein, A. I. Larkin, and V. M. Vinokur, Rev. Mod. Phys. **66**, 1125 (1994).
[11]M. Tachiki and S. Takahashi, Solid State Commun. **72**, 1083 (1989).
[12]T. Matsushita, *Flux Pinning in Superconductors* (Springer-Verlag, Berlin, 2007), p. 155.
[13]R. P. Huebener, *Magnetic Flux Structures in Superconductors* (Springer-Verlag, Berlin, 1979), p. 121.
[14]M. Tinkham, Phys. Rev. **129**, 2413 (1963).